ChemComm

Accepted Manuscript

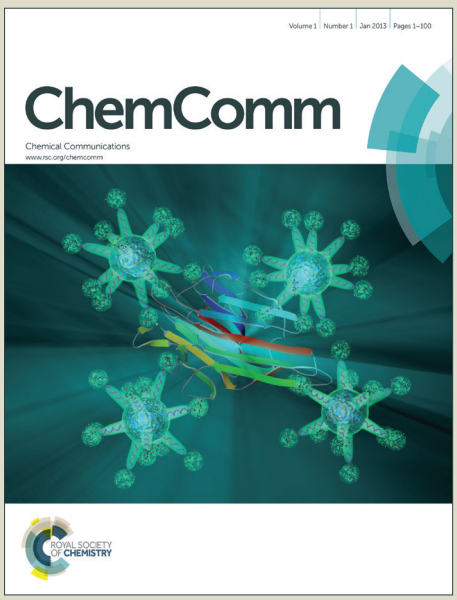

ROYAL SOCIETY OF CHEMISTRY

www.rsc.org/chemcomm

Journal Name

RSCPublishing

COMMUNICATION

Extending Shell-Isolated Nanoparticle-Enhanced Raman Spectroscopy Approach to Interfacial Ionic Liquids at Single Crystal Electrode Surfaces

Cite this: DOI: 10.1039/xoxxoooooox

Received ooth January 2012,
Accepted ooth January 2012

DOI: 10.1039/xoxxoooooox

www.rsc.org/

Meng Zhang, Li-Juan Yu, Yi-Fan Huang, Jia-Wei Yan, Guo-Kun Liu, De-Yin Wu,* Zhong-Qun Tian and Bing-Wei Mao*

We employ for the first time shell-isolated nanoparticle-enhancement strategy to extend Raman spectroscopic study to single crystal electrode surfaces in ionic liquids, and combine density functional theory (DFT) calculations to elucidate the structural details of the imdazolium-based ionic liquid-Au single crystal electrode interfaces.

Understanding the structure of electrode/electrolyte interface is one of the most important tasks of modern electrochemistry, which provide basis for precise correlation of structure and properties of electrochemical processes taking place at the interface.[1,2] Room temperature ionic liquids (ILs), which can serve as electrochemical solvents because of wide electrochemical window, high conductivity, low volatility and thermal stability, have found wide applications in electrochemistry such as electrodeposition and energy devices.[3-10] However, the electrochemical interfaces in ionic liquids are very complicated because of the involvement of strong interactions between highly concentrated solvent ions and electrode surfaces, and require adequate molecule-level experimental and theoretical investigations for which well-defined single crystal electrodes serve as ideal systems to gain a clear picture about the interfaces.[11]

In-situ microscopy and force spectroscopy have been employed to investigate single crystal electrode/ILs interfaces. Among these works, high-resolution scanning tunnelling microscopy (STM) studies[12-17] have revealed detailed surface adsorption structures of anions and cations, while potential-dependent force curve measurements by atomic force microscope (AFM)[18] have demonstrated the existence of layered structure of ionic liquids near electrodes surface. However, STM and AFM are lack of chemical sensitivity, and further elucidation of the adsorbate-surface interaction and adsorbate orientation/configuration relies on the application of energy-resolved spectroscopic techniques. Some studies employing Fourier transform infrared reflection spectroscopy (FTIRAS),[19] surface enhanced infrared adsorption spectroscopy (SEIRAS),[20] sum frequency generation (SFG)[21,22] and surface enhanced Raman spectroscopy (SERS)[23-27] suggest the orientation change of imidazolium rings from vertical-standing to flat-lying at Pt, Cu and Ag electrode surfaces as the potentials are made more negatively.

Despite the fact that a number of studies have already been devoted to the electrochemical interfaces in ionic liquids, understanding of the interfacial structure is still in the infant stage. Up to now all of the spectroscopic studies including the above mentioned works exclusively use polycrystalline or rough surfaces, which impose complexity on data analysis and difficulty in correlation of results with those obtained by STM and AFM on single crystal electrodes. The detailed adsorption configuration such as the tilted adsorption cannot be well studied on rough surfaces.

The main barrier for spectroscopic investigations on atomically flat single crystal electrodes is that the signals are usually very weak. This is especially the case for Raman spectroscopy. However, this situation may be changed using shell-isolated nanoparticle enhanced Raman spectroscopy (SHINERS) developed by Tian and co-workers.[28] They have demonstrated power of SERS detection of molecules on smooth single crystalline electrodes in aqueous solutions. SHINERS utilizes the electromagnetic enhancement provided by Au nanoparticle cores which are isolated by an ultrathin silica shell. Valuable mechanistic information about surface processes has been obtained.[29-35] However, interfacial studies of ionic liquids on single crystalline electrodes by SHINERS are more challenging than those in aqueous solutions because the strong signals from bulk ionic liquids would interfere the detection of Raman signals of the weak interfacial ionic liquid species on single crystal electrodes. In addition, the assignments of vibrational modes of ionic liquid molecules are not straight forward and rely on the theoretical guidance.

In this work, we extend SHINERS to Au single crystal electrodes in ionic liquid (as shown in Figure 1) and combine DFT calculations to elucidate the structural details of the interface in ILs. Though challenging, potential-dependent Raman spectra of ILs with different alkyl side chain lengths, namely 1-butyl-3-methylimidazolium hexafluorophosphate ($BMIPF_6$) and 1-octyl-3-methylimidazolium hexafluorophosphate ($OMIPF_6$), have been obtained in a wide potential range. Density functional calculations of vibrational spectra as well as orientation-dependent polarizability tensors of certain vibration modes of BMI^+ are also carried out to assist accurate assignments of vibrational bands and orientation analysis of the cations. The combined SHINERS-DFT studies of ILs at structurally well-defined surface shine light on the complicated interfacial structure in ILs.

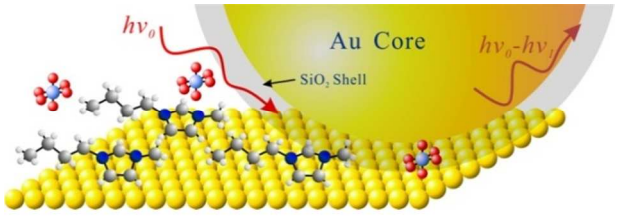

Figure 1. Schematic diagram of the SHINERS experiment in ILs.

The Raman spectrum of the bulk $BMIPF_6$ is displayed in Figure 2b. The band at 740 cm^{-1} is attributed to the symmetric stretching mode of PF_6^- anion, while the bands in 1000~1600 cm^{-1} and 2700~3300 cm^{-1} regions originate from of BMI^+ cation. These basic spectral features are similar to those reported in the literatures.[36,37] By comparing the spectrum with that of bulk $OMIPF_6$, Figure 2c, the band at 2974 cm^{-1} can be assigned to the stretching of C-H (C6) from the methyl group while the three bands at 2880, 2919 and 2944 cm^{-1} are from the C-H stretching of the butyl group.

Detailed assignments of the bands located at 1000~1600 cm^{-1} are not straightforward, and therefore DFT calculations of Raman spectra are applied to BMI^+ to guide the assignments. Figure 2a shows the calculated spectrum of BMI^+, which agrees reasonably well with the experimentally measured one in this region. Tentative assignments are given in Table S1. Worth of mentioning is that the weak band at 1306 cm^{-1} and the broad band around 1450 cm^{-1} are assigned, respectively, to the twisting and scissoring of CH in butyl, while the bands at 1340,1390,1420 and 1568 cm^{-1} are the integrated imidazolium ring vibrations containing components from C-N and C-C bonds stretching. The bands at 1568 and 3184 cm^{-1} are related to the stretching of C4-C5 and H-C4C5-H of the HC=CH group in the BMI^+ ring.

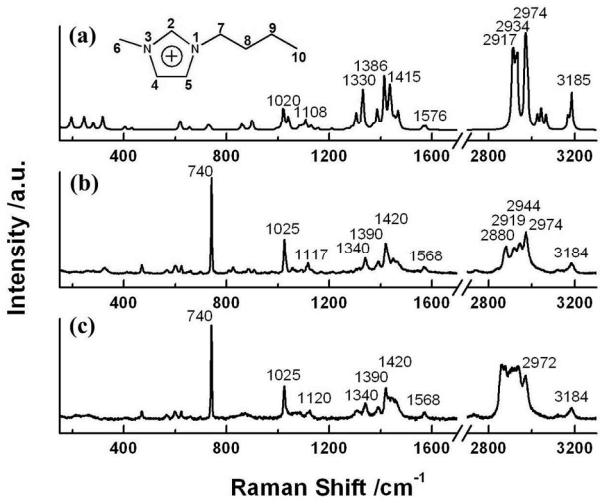

Figure 2. Raman spectra of (a) BMI^+ calculated at the B3LYP/6-311+G(d,p) level, (b) bulk $BMIPF_6$ and (c) bulk $OMIPF_6$.

The CVs of Au(111) in $BMIPF_6$ and $OMIPF_6$ (Figure S2) show that both the ionic liquids have wide potential windows. In-situ SHINERS measurements are conducted on Au(111) in $BMIPF_6$ first in a wide potential region (-2.4 V ~ +0.8 V) across the potential of zero charge (PZC) of the system (-0.1 V),[18] Figure 3. At potentials positive of PZC, where anion PF_6^- is expected to adsorb, the surface Raman spectra appear similar with that of the bulk phase and almost independent of potential, meaning that the interaction of PF_6^- with

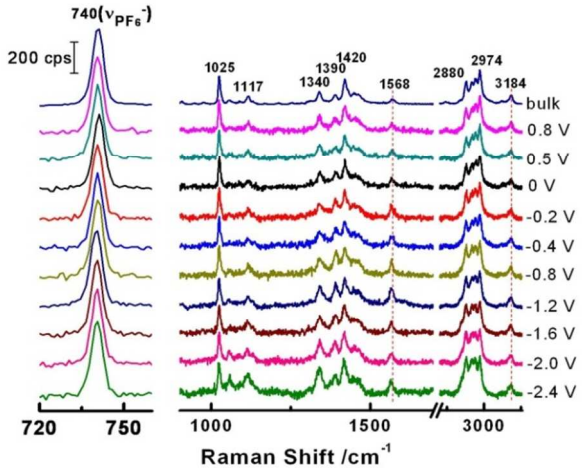

Figure 3. Potential-dependent Raman spectra of $BMIBF_6$ on Au(111) covered with Au@SiO_2 NPs. Laser power: 2 mW; collecting time: 10s.

the Au surface is weak. Noteworthy is that the insensitive potential dependency of the Raman band of BF_4^- anion is also observed in the SERS study on Cu electrode by Rubim and co-workers.[25]

Weak yet obvious potential-dependence of intensity and Raman shift of some vibration from BMI^+ are observed at potentials negative of PZC, Figure 3, which disclose information valuable to structural analysis of the interface. Two pieces of information are brought to attention: First, the bands associated with stretching of C4-C5 and H-C4C5-H of the HC=CH group in the BMI^+ ring shift to 1562 cm^{-1} and 3176 cm^{-1} at -2.4 V (Figure 4a and 4b), respectively, while all other bands of $BMIPF_6$ remain unchanged with decreasing potential, Figure 3, suggesting that the BMI^+ interacts with the Au electrode through the HC4C5H side of the ring. Second, the intensity of the bands at 1340 and 1390 cm^{-1} related to the imidazolium ring and the bands at 1115, 2880, 2919 and 2944 cm^{-1} related to the butyl group show stronger intensity at decreasing potentials, indicating BMI^+ is located closer to the electrode surface at negatively charged surface. The most eye-catching feature of the intensity vs. potential curve in the potential region negative of PZC is that the intensity of the 1340 cm^{-1} band increases monotonically while the 1390 cm^{-1} band shows a maximum upon decreasing potential, Figure 4c. The difference in the trends of intensity change of these bands implies orientation change of the BMI^+ on the Au surface.

However, usual approach to analyze the orientation at different potentials, which is based on simple comparison of in-plane and out-of-plane vibrations of an aromatic ring, is not applicable because the bands of the BMI^+ ring are integrated contributions from complicated components of vibration modes (as shown in Table SI). Alternatively, we perform DFT calculation to analyze the potential-dependent orientation of BMI^+ at the surface by inspecting the influence of the optical electric field on the Raman intensities of certain vibrational modes of the molecule. By fixing the optical electric field perpendicular to the Au surface, we rotate the plane of BMI^+ ring by varying the dihedral angle between the ring plane and Au surface at fixed HC4C5H side. The polarizability tensors, α_{zz}, of the stretching modes at 1340 and 1390 cm^{-1} of the molecule at six typical dihedral angles are calculated and presented in Figure 4d. Detailed descriptions are provided in the supporting materials.

On the basis of modelling results, we highlight the results which favour the orientation analysis as follows: When the BMI^+ ring plane orients from flat to vertical configuration with the corresponding

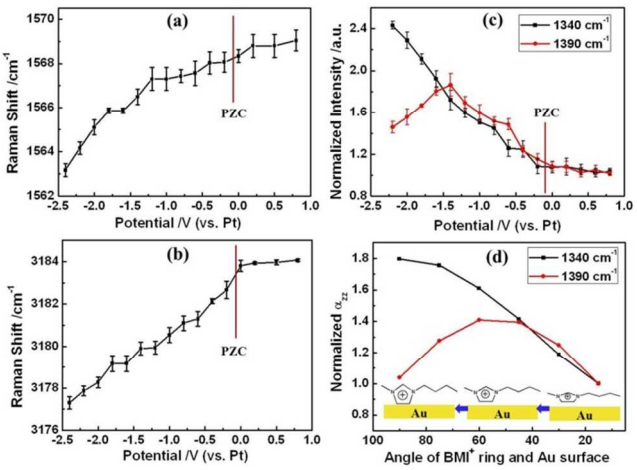

Figure 4. Potential-dependent Raman shift of (a) 1568 cm^{-1} band, (b) 3184 cm^{-1}band and(c) potential-dependent normalized intensity of 1340 and 1390 cm^{-1} bands of $BMIPF_6$ on Au(111); (d) Calculated α_{zz} of 1340 and 1390 cm^{-1} stretching modes with different orientations of BMI^+.

dihedral angle between the imidazolium ring and Au surface changing from 15° to 90°, the α_{zz} of 1340 cm^{-1} band gradually increases while the α_{zz} of 1390 cm^{-1} band displays a maximum at around 60°, as shown in Figure 4d. This trend is consistent with the experimental results at negatively charged surface, Figure 4c, which allows us to propose that the orientation of BMI^+ on Au(111) surface in the potential region negative of PZC change from lying nearly parallel to the surface at less charged surface to tilted configuration with the HC4C5H interacting with the surface and finally up-standing on the surface at more negative potentials.

By comparing the experimental results and DFT calculations presented above, a model of potential dependent interfacial structure of Au single crystal electrode/imidazolium-based ILs is proposed in Figure 5: At positively charged surface, anions adsorb on the surface with weak electrostatic interaction, Figure 5a, while cations are

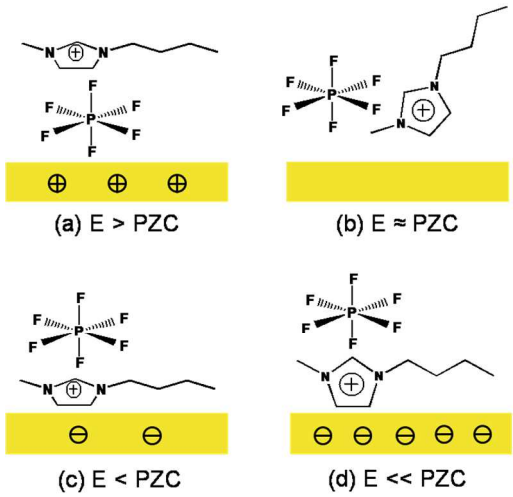

Figure 5. Proposed interfacial structure of Au single crystal electrode/imidazolium-based ionic liquid at different potential regions: (a) positive of PZC, (b) near PZC, (c) negative of PZC and (d) more negative of PZC.

located close to the anions in the solution side so that the Raman spectra are similar to that of the bulk. At the potential close to PZC, neither cations nor anions adsorb at the surface significantly, Figure 5b. However, as the surface becomes negatively charged, the cation adsorbs on the surface, starting with a nearly flat configuration, Figure 5c, to tilted and finally vertical configurations with the HC4C5H interacting with the surface at decreasing potential, Figure 5d.

Noteworthy is that the flat-flying configuration of BMI^+ in the initial stage of adsorption facilitate strong interaction between the imidazolium ring and Au surface, which would in turn weaken the inter-atomic interaction of the surface Au atoms. This provides a possible explanation for the etching of Au surface in this potential region observed by STM in our previous study.[17] The slightly tilted adsorption configuration is likely associated with the double-row structure in the "worm-like" structure. In addition, by changing of cation orientation from flat-lying to tilted and finally vertical configuration, the coverage of adsorbed cations increases, which is necessary to balance the increasing negative charge of the surface.

The in-situ SHINERS experiments have also been performed on Au(100) in $BMIPF_6$ and Au(111) in $OMPF_6$ to inspect the influence of surface structure and alkyl side chain length of imidazolium cations on the adsorption orientation of ILs, Figure S3~6. The main features of the potential dependency of the intensity of $BMIPF_6$ on Au(100) are similar to those on Au(111), which indicate the adsorption configurations on the two single crystal electrodes are essentially the same. For $OMPF_6$ on Au(111), the potential-dependency of intensity of the bands at 1340 and 1390 cm^{-1} and the Raman shift of the bands at 1568 and 3184 cm^{-1} are similar to those of $BMIPF_6$ on Au(111), indicating that the orientation of OMI^+ is basically the same as that of BMI^+ on Au(111), and the side chain length of the cation does not influence the adsorption configuration.

In conclusion, we have extended Raman spectroscopic study into electrochemical interfaces in ionic liquids on atomically smooth Au single crystal surfaces by employing shell-isolated nanoparticle-enhancement strategy. The potential-dependent Raman spectra obtained in a wide range of potential across PZC disclose information valuable to structural analysis of the interface with the support of DFT calculations: At potentials positive of PZC, PF_6^- anion adsorbs at the surface via very weak electrostatic interaction, thus showing almost bulk-like Raman spectra. At potentials negative of PZC, BMI^+ interacts with the surface through the HC4C5H groups of the ring, adopting configurations from flat-lying, gradual up-leaning, and finally vertical-standing along with decreasing potentials. The combined SHINERS-DFT approach for single crystal electrode surfaces demonstrated in the present work provides opportunities for in-depth investigations of various ionic liquid interfaces as SHINERS can be applied to virtually all kinds of solid materials.[28]

Notes and references

*State Key Laboratory of Physical Chemistry of Solid Surfaces and Department of Chemistry, College of Chemistry and Chemical Engineering, Xiamen University, Xiamen 361005, China.
Emails: bwmao@xmu.edu.cn; dywu@xmu.edu.cn.

This work is supported by MOST (No. 2012CB932902) and National Science Foundation of China (No. 21033007, 21021002)

†Electronic Supplementary Information (ESI) available: [EC-Raman experiments and DFT calculation details]. See DOI: 10.1039/c000000x/

1 D. M. Kolb, *Angew. Chem. Int. Ed.*, 2001, **40**, 1162.

2 V. Climent and J. M. Feliu, *J. Solid State Electrochem.*, 2011, **15**, 1297
3 T. Welton, *Chem. Rev.*, 1999, **99**, 2071.
4 M. C. Buzzeo, R. G. Evans and R. G. Compton, *ChemPhysChem*, 2004,**5**, 1106.
5 F. Endres and S. Z. El Abedin, *Phys. Chem. Chem. Phys.*, 2006, **8**, 2101.
6 P. Hapiot and C. Lagrost, *Chem. Rev.*, 2008, **108**,2238.
7 M. Armand, F. Endres, D. R. MacFarlane, H. Ohno andB. Scrosati, *Nat Mater*, 2009, **8**, 621.
8 H. T. Liu, Y. Liu and J. H. Li,*Phys. Chem. Chem. Phys.*, 2010, **12**, 1685.
9 Y. Z. Su, Y. C. Fu,Y. M. Wei, J. W. Yan and B. W. Mao, *ChemPhysChem*, 2010,**11**, 2764.
10 R. Kawano, T. Katakabe, H. Shimosawa, M. KhajaNazeeruddin, M. Gratzel, H. Matsui, T. Kitamura, N. Tanabe and M. Watanabe, *Phys. Chem. Chem. Phys.*, 2010, **12**, 1916.
11 M. V. Fedorov and A. A. Kornyshev, *Chem. Rev.*, 2014, **114**, 2978.
12 L. G. Lin, Y. Wang, J. W. Yan, Y. Z. Yuan, J. Xiang and B. W. Mao,*Electrochem. Commun.*, 2003, **5**, 995.
13 G.B. Pan and W.Freyland, *Chem. Phys. Lett.*, 2006, **427**, 96.
14 Y. Z. Su, Y. C. Fu,J. W. Yan, Z. B. Chen and B. W. Mao, *Angew. Chem.Int. Ed.*, 2009, **48**, 5148.
15 M. Gnahm, C. Muller, R. Repanszki, T. Pajkossy and D. M. Kolb, *Phys. Chem. Chem. Phys.*, 2011, **13**, 11627.
16 Y. Z. Su, J. W. Yan, M. G. Li, M. Zhang and B. W. Mao, *J. Phys. Chem. C*, 2012, **117**, 205.
17 Y. Z. Su, J. W. Yan, M. G. Li, Z. X. Xie, B. W. Mao and Z. Q. Tian, *Z. Phys. Chem.*, 2012, **226**, 979.
18 X. Zhang, Y. X. Zhong, J. W. Yan, Y. Z. Su, M. Zhang and B. W. Mao, *Chem. Commun.*, 2012, **48**, 582.
19 N. Nanbu, Y. Sasaki and F. Kitamura, *Electrochem. Commun.*, 2003, **5**, 383.
20 N. Nanbu, T. Kato, Y. Sasaki and F. Kitamura, *Electrochemistry*, 2005, **73**, 610.
21 S.Rivera-Rubero and S. Baldelli, *J. Phys. Chem. B*, 2004, **108**, 15133.
22 S. Baldelli, *Acc. Chem. Res.*, 2008, **41**, 421.
23 V.O. Santos, M. B. Alves, M. S. Carvalho, P. A. Z. Suarez and J. C.Rubim, *J. Phys. Chem. B*, 2006, **110**, 20379.
24 J. C. Rubim, F. A. Trindade, M. A. Gelesky, R. F. Aroca and J. Dupont, *J. Phys. Chem. C*, 2008, **112**, 19670.
25 C. R. R. Brandão,L. A. F. Costa, H. S. Breyer and J. C. Rubim, *Electrochem.Commun.*, 2009, **11**, 1846.
26 Y. X. Yuan, T. C. Niu, M. M. Xu, J. L. Yao and R. A. Gu, *J. Raman Spectrosc.*, 2010,**41**, 516.
27 T. C. Niu, Y. X. Yuan, J. L. Yao, F. Lu and R. A.Gu, *Sci. China Chem.*, 2011, **54**, 200.
28 J. F. Li, Y. F. Huang, Y. Ding, Z. L. Yang, S. B. Li, X. S. Zhou, F. R. Fan, W. Zhang, Z. Y. Zhou, Y. W. De, B. Ren, Z. L. Wang andZ. Q. Tian, *Nature*, 2010, **464**, 392.
29 J. R. Anema, J. F. Li, Z. L. Yang, B. Ren and Z. Q. Tian, *Annu. Rev. Anal. Chem.*, 2011, **4**, 129.
30 Y. F. Huang, C. Y. Li, I. Broadwell, J. F. Li, D. Y. Wu, B. Ren and Z. Q. Tian, *Electrochim. Acta*, 2011, **56**, 10652.
31 J. F. Li, S.Y. Ding, Z. L. Yang, M. L. Bai, J. R. Anema, X. Wang, A. Wang, D. Y. Wu, B. Ren, S. M. Hou, T. Wandlowski and Z. Q. Tian, *J. Am. Chem. Soc.*, 2011, **133**, 15922.
32 B. Liu, A. Blaszczyk, M. Mayor and T. Wandlowski, *ACS Nano*, 2011, **5**, 5662.
33 D. P. Butcher, S. P. Boulos, C. J. Murphy, R. C. Ambrosio and A. A. Gewirth, *J. Phys. Chem. C*, 2012, **116**, 5128.
34 N. R. Honesty and A. A. Gewirth, *J. Raman Spectrosc.*, 2012, **43**, 46.
35 J. F. Li, A. Rudnev, Y. C. Fu, N. Bodappa and T. Wandlowski, *ACS Nano*, 2013, **7**, 8940.
36 E. R. Talaty, S. Raja, V. J. Storhaug, A. Dölle and W. R. Carper, *J. Phys. Chem. B*, 2004, **108**, 13177.
37 R. W. Berg, *Monatsh. Chem.*, 2007, **138**, 1045.

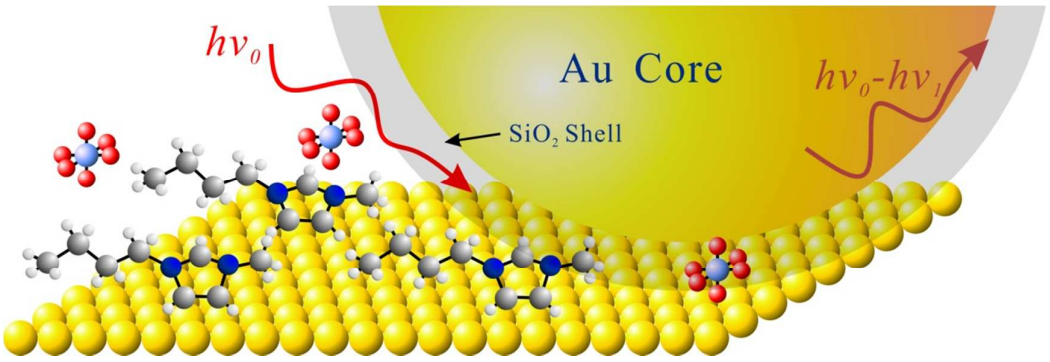

We employ for the first time shell-isolated nanoparticle-enhancement strategy to extend Raman spectroscopic study to single crystal electrode surfaces in ionic liquids, and combine density functional theory (DFT) calculations to elucidate the structural details of the imdazolium-based ionic liquid-Au single crystal electrode interfaces.